© Universiti Tun Hussein Onn Malaysia Publisher's Office

IJIE

Journal homepage: http://penerbit.uthm.edu.my/ojs/index.php/ijie
ISSN : 2229-838X e-ISSN : 2600-7916

The International Journal of Integrated Engineering

Synthesis and Structural Study of a Novel $La_{0.67}Ca_{0.33}Cr_{0.9}Cu_{0.1}O_{3-\delta}$ Anode for Syngas-Fuelled Solid Oxide Fuel Cell

Nikdalila Radenahmad, Ahmed Afif, Md Sumon Reza, Shammya Afroze, Jun-Young Park, Juliana Zaini, Juntakan Taweekun, Abul Kalam Azad

[1]Faculty of Integrated Technologies,
Universiti Brunei Darussalam, Jalan Tunku Link, Gadong BE 1410, BRUNEI DARUSSALAM

*Corresponding Author

DOI: https://doi.org/10.30880/ijie.2021.13.07.008
Received 21 October 2020; Accepted 23 March 2021; Available online 30 September 2021

Abstract: Solid oxide fuel cell (SOFC) is an alternative energy generation device that converts chemical energy into electrical energy from the use of hydrogen or hydrogen-rich fuel. A light hydrocarbon, e.g. methane (CH_4), is a hydrogen-rich fuel that can be used as an alternative fuel to hydrogen in SOFC application. Carbon-containing fuel is accessible from natural gas, biogas, biomass gasification, etc. Biomass gasification produces methane, hydrogen (H_2), etc. as syngas products which could be integrated with SOFC. As anode is an outer layer of SOFC which exposes to fuel, the development of anode for carbon-containing fuel application is essential. Conventional Ni-containing anode is found to create carbon deposition which degrades the cell. The replacement of copper (Cu) to Ni has been studied to enhance the direct electrochemical oxidation of dry hydrocarbons which is free from carbon deposition. With the interest of Cu doping, a La-based anode has been doped with 10 % Cu at B-site of perovskite structure as $La_{0.67}Ca_{0.33}Cr_{0.9}Cu_{0.1}O_{3-\delta}$ and studied the X-ray diffraction (XRD), scanning electron microscope (SEM) and energy dispersive X-ray (EDX) for future application in syngas-fuelled SOFC.

Keywords: Synthesis, anode, glycine nitrate synthesis, solid oxide fuel cell, syngas, Rietveld refinement

1. Introduction

The fuel cell is an alternative energy generation device that converts chemical energy into electrical energy with low or zero-emission, high efficiency and quiet operation. Solid oxide fuel cell (SOFC) is a category of fuel cell that has been fabricated by oxide-type materials. SOFC comprises a dense layer (electrolyte) sandwiched between two porous layers (an anode and a cathode). The conventional SOFC is operable at high temperatures (700 – 1,000 °C) which promotes the internal reforming mechanism to utilize a wide range of fuels including hydrogen, hydrogen-rich fuel, hydrocarbons, natural gas or biogas. The biomass gasification process is a source that produces methane (CH_4), hydrogen (H_2), etc. as syngas products that could be utilized as fuels in SOFC [1],[2]. The integration of biomass gasification and SOFC has been widely studied for electricity generation [3],[4]. The syngas-fuelled SOFC has got an interest in the use of alternative fuels apart from only pure H_2.

Anode reactions:

$$H_2 + O^{2-} \rightarrow H_2O + 2e^- \quad (1)$$
$$CH_4 + 3O^{2-} \rightarrow CO + 2H_2O + 6e^- \quad (2)$$
$$CH_4 + 4O^{2-} \rightarrow CO_2 + 2H_2O + 8e^- \quad (3)$$

*Corresponding author: abul.azad@ubd.edu.bn

$$CH_4 \rightarrow C + 2H_2 \quad (4)$$
$$C + O^{2-} \rightarrow CO + 2e^- \quad (5)$$
$$C + 2O^{2-} \rightarrow CO_2 + 4e^- \quad (6)$$

Cathode reaction:

$$O_2 + 4e^- \rightarrow 2O^{2-} \quad (7)$$

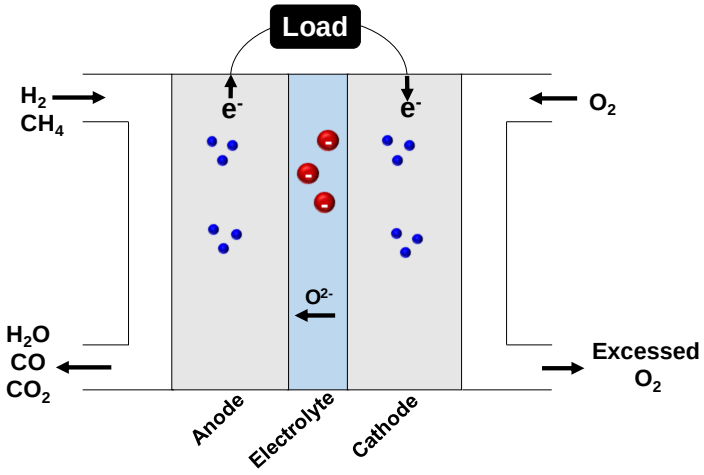

Fig. 1 - Diagram of oxygen ion conduction and overall process in H_2/CH_4-fuelled SOFC

The typical SOFC can be seen in Fig. 1 when H_2 and CH_4 are used as fuels. The possible chemical reactions in H_2 or CH_4-fuelled SOFC are as equations (1) – (7) [5]. When carbon-containing fuel is fed to SOFC, there exists carbon deposition at the anode. However, material development especially anode is the crucial approach to prevent coke formation [6].

1.1 The Development of Anode Material

The anode is generally categorized into two main classes: Ni-based anode and Ni-free anode. The Ni-based anode consists of nickel in compound with superior properties in catalytic activity, electrical conductivity, gas diffusivity and structural integrity such as Ni/YSZ, Ni/ScSZ, Ni/rare earth, Ni/Yttrium doped Ceria. YSZ has been fabricated into Ni/YSZ as a favoured anode by its high electrochemical mechanism in H_2 oxidation with the high stability under SOFC operation [7] but Ni/YSZ suffers from coke formation when carbon-containing fuel is used. The carbon formation can occur more probably on Ni-based materials compared to other anode materials (Ni-free anode).

The Ni-free anode is the cermet that is free of nickel in the compound. It is an alternative anode for SOFC application with carbon-containing fuel. There existed the Ni-free anode development of $SrMoO_4$ [8], $Sr_2Mg_{1-x}Mn_xMoO_{6-\delta}$ [9], Sr_2CoMoO_6 [10], RuO_x–ZrO_2 [11] and $Gd_2Ti_{1.4}Mo_{0.6}O_{7-\delta}$ [12] tested in H_2, CH_4 and H_2S. The reported studies have been successfully carried out on Cu-ceria [13], Cu–YSZ [13] and Cu–CeO_2–ScSZ [14] in a carbon-containing atmosphere. A Cu/CeO_2/YSZ anode shows better performance with CO and syngas fuels compared with Ni/YSZ. A copper (Cu) doping in Cu/CeO_2/YSZ composite anode can be a solution to prevent carbon deposition by its direct electrochemical oxidation of dry hydrocarbons [15]. When Ni is replaced by impregnating ceria with Cu, the reaction (8) does not take place on Cu and the availability of O^{2-} on the surface of the ceria assists the reactions (9) and (10) over the reaction (11). This overcomes the coke formation [15].

$$CH_4 + 2O^{2-} = C + 2H_2O + 4e^- \quad (8)$$
$$CO + O^{2-} = CO_2 + 2e^- \quad (9)$$
$$CO + H_2O = CO_2 + H_2 \quad (10)$$
$$2CO = C + CO_2 \quad (11)$$

A number of studies on La-based anodes, such as $LaFe_{0.5}Cr_{0.5}O_3$ [16] and $La_{0.83}(Ba,Ca)_{0.17}Fe_{0.5}Cr_{0.5}O_{3-\delta}$ [17] have been carried out especially $La_{1-x}Sr_xCr_{1-y}Ru_yO_3$ [18], $La_{0.8}Sr_{0.2}CrO_3$ based Ru catalysts [19], $(La_{0.75}Sr_{0.25})Cr_{0.5}Mn_{0.5}O_{3-\delta}$ [20], $La_{0.8}Sr_{0.2}Cr_{0.8}Mn_{0.2}O_{3-\delta}$ [21] and $La_{1-x}Ca_xCr_{0.5}Ti_{0.5}O_{3-\delta}$ [22] were tested in carbon-containing atmospheres. With the interest in Cu doping La-based anode, we synthesized a Cu-dopping in $La_{0.67}Ca_{0.33}Cr_{0.9}Cu_{0.1}$ (LCCC) as a novel anode for application in syngas-fuelled SOFC.

2. Experimental

A composite anode of $La_{0.67}Ca_{0.33}Cr_{0.9}Cu_{0.1}$ (LCCC) was synthesized by the glycine nitrate process (GNP) method. The stoichiometric ratio of $La(NO_3)_3{\cdot}6H_2O$, $CaN_2O_6{\cdot}4H_2O$, $CrN_3O_9{\cdot}9H_2O$, $Cu(NO_3)_2{\cdot}2.5H_2O$ and glycine (fuel) were placed in a beaker in the ratio of 1:2 (nitrates: fuel). The mixture was dissolved in an amount of deionized (DI) water in a beaker and stirred with a magnet stick on a magnetic heater at 280 °C. The mixing was monitored until the auto-combustion took place and the mixture becomes ash. The obtained ash was used to calcine at 600 °C for 4 hours. The powder was ground with acetone until it dried and calcined for the second time at 1,000 °C for 4 hours. X-ray diffractometer of Empyrean Alpha 1 of Malvern Panalytical (CuKα1 = 1.5406 Å) was used at Sejong University to examine the crystalline phase in the air and performed Rietveld analysis by FullProf software [23]. The morphology of the material was studied by scanning electron microscope (SEM) of JEOL JSM-7610F at Universiti Brunei Darussalam to observe the micro-scale feature of the material. The solid materials were placed on the sample holder and conducted carefully to analyzing the chamber that was controlled the pressure in JEOL. The device employed electron dispersion to perform an SEM image on a computer screen connected. A device to identify the elemental distribution is an energy dispersive X-ray (EDX) analyzer. EDX displays the content of the elements in percentage. The EDX utilizes an effective X-ray to detect the chemical compositions of the sample.

3. Results and Discussion

Fig. 2a) shows the XRD profile of LCCC and Fig. 2b) displays the Rietveld refinement by using FullProf. The indexing of the XRD was carried out using the software TREOR90. The Rietveld refinement reveals that LCCC is an orthorhombic symmetry (space group of *Pbnm*). The diagram of the 3D atomic structure is shown in Fig. 3. In perovskite LCCC, La and Ca (purple atoms) reside at A-site surrounded with octahedral (BO_6) and oxygen atoms (red atoms) at the corners. The atoms of Cr and Cu (green atoms) reside at the B-site at the centre of each octahedral. LCCC has parameters as shown in Table 1.

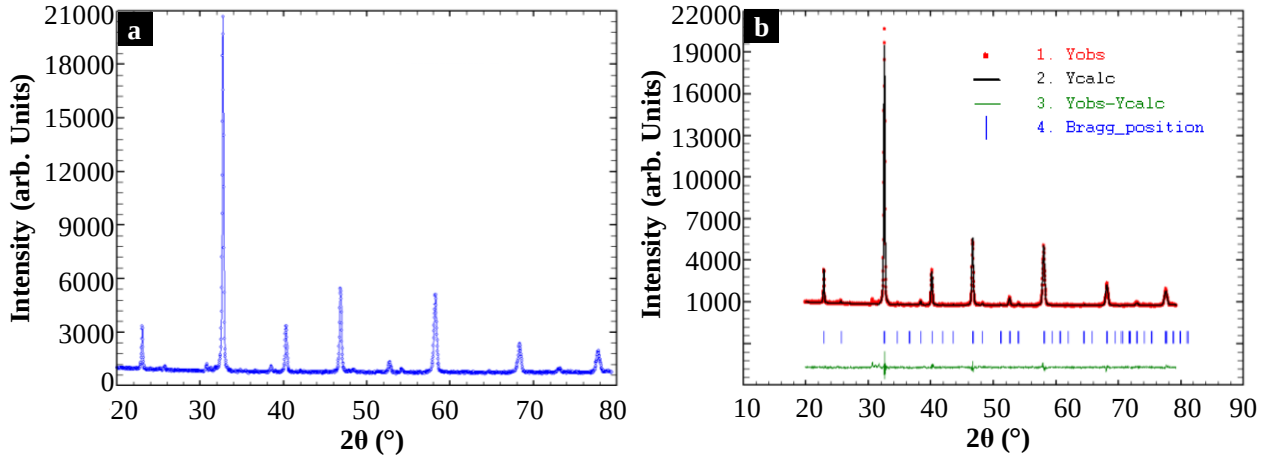

Fig. 2 - (a) XRD profile of LCCC; (b) Rietveld refinement profile of LCCC where the observed data is in red dot and calculated data is in the continuous black line. The short blue vertical lines represent the position of the Bragg reflections. The bottom green line shows the difference between plots (J_{obs}-I_{calc})

The cell parameters of $La_{0.67}Ca_{0.33}Cr_{0.9}Cu_{0.1}O_{3-\delta}$ (a = 5.5043 Å, b = 5.4914 Å and c = 7.7728 Å) are comparable to values of orthorhombic $La_{0.75}Sr_{0.25}Cr_{0.5}Mn_{0.5}O_{3-\delta}$ (a = 5.5028(4) Å, b = 5.4823(5) Å and c = 7.7686(1) Å). In a report, $(La_{0.75}Sr_{0.25})_{1-x}Cr_{0.5}Mn_{0.5}O_{3-\delta}$ ($0 \leq x \leq 0.1$) was synthesized in different firing conditions (dwelling time, gas condition) which affect the lattice setting in different space groups (hexagonal, orthorhombic, tetragonal, cubic) [20]. The obtained cell parameters of LCCC in this study are also comparable with a very similar composition of $La_{0.8}Ca_{0.2}Cr_{0.5}Ti_{0.5}O_{3-\delta}$ (a = 5.4887(2) Å, b = 5.4777(2) Å and c = 7.7433(3) Å) as the same orthorhombic phase (*Pbnm*). The obtained unit cell volume of LCCC is 234.9(0.046) $Å^3$ which is in agreement with 232.81(3) $Å^3$ of $La_{0.8}Ca_{0.2}Cr_{0.5}Ti_{0.5}O_{3-\delta}$. In $La_{1-x}Ca_xCr_{0.5}Ti_{0.5}O_{3-\delta}$, the atoms crystallized in rhombohedral when the Ca ratio is 0 and 0.1 while it is two perovskite-like phases when the Ca portion is 0.2. The $La_{0.8}Ca_{0.2}Cr_{0.5}Ti_{0.5}O_{3-\delta}$ is rather rhombohedral than orthorhombic or the amount of the rhombohedral phase is larger compared with the orthorhombic phase [22]. A-site of perovskite can be doped with the large ionic radius element and B-site can be doped with the small ionic radius element [24]. It is reasonable to infer that a small percentage of Cu in $La_{0.67}Ca_{0.33}Cr_{0.9}Cu_{0.1}$ resides at B-site with Cr due to the similar ionic radius of Cr (0.615 Å) and Cu (0.73 Å) in 6-octahedron coordination while larger ionic radius elements, La (1.36 Å) and Ca (1.34 Å) in 12-cuboctahedral coordination, reside at A-site [25].

Microstructure plays a very important role in the properties of the material. Fig. 4 shows the SEM image of the LCCC. The sample displays a porous feature as a requirement of the anode. In addition, the surface exhibited no visible crack which suggests the stability of the anode at the final sintering temperature of 1,000 °C. In a complete fuel cell, the porosity in the electrode allows the fuel to transport through the hole and exchange electrons and ions at the surface of the material as equations (1)-(7). Electron transportation results in electricity generation. Therefore, anode or cathode is necessary to be porous while electrolyte is a dense layer. LCCC exhibits the well-connecting grains in the size of 1-3 µm. EDX analysis of the sample reveals the presence of La, Ca, Cr, Cu and O. The elemental compositions of LCCC are shown in Table 2 with the comparison between EDX source and formula source. The results from the EDX source are reasonably comparable to formula source values because X-ray is an effective medium to detect the elements of compounds accurately. The uses of X-Ray exist in XRD and EDX, this confirms that X-ray is the efficient media to identify the elements of the material. La, Cr and O are the main elements in perovskite (ABO_3) hence the weight percentages are larger than Ca and Cu.

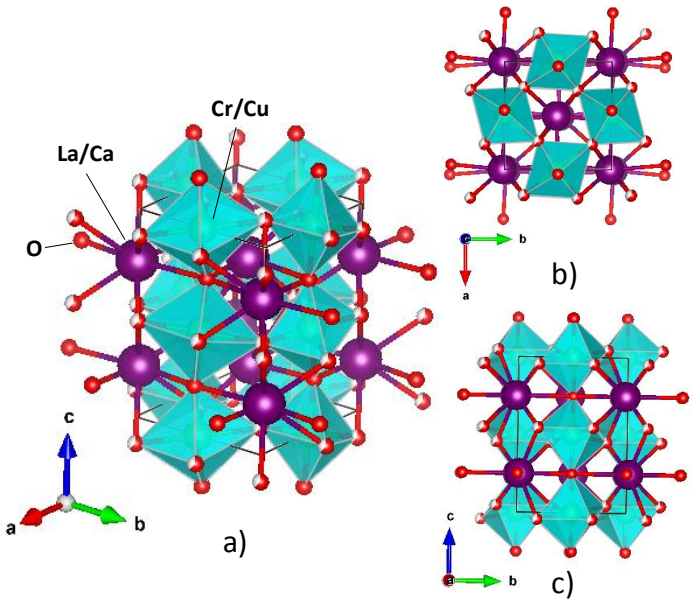

Fig. 3 - Schematic 3D diagram of perovskite (ABO_3) structure of LCCC which was drawn by Vesta software in (a) overall view; (b) top view; (c) front view

Table 1 - Summary of the Rietveld refinement results for $La_{0.67}Ca_{0.33}Cr_{0.9}Cu_{0.1}O_{3-\delta}$ using the space group *Pbnm*

Parameters	Detail
Space group	*Pbnm*
Cell parameters	
a	5.504 Å
b	5.491 Å
c	7.773 Å
alpha = beta = gamma	90 °
Volume	234.945(6) $Å^3$
Density	6.049 g/cm^3
Atomic position (x y z)	
La	0.00051 0.01809 0.25000
Ca	0.00051 0.01809 0.25000
Cr	0.50000 0.00000 0.00000
Cu	0.50000 0.00000 0.00000
O1	0.04517 0.49563 0.25000
O2	0.73652 0.31600 0.04523
R-factors	
Rp	17.0
Rwp	12.1
Chi^2	2.05

4. Conclusion

A novel perovskite-type anode, $La_{0.67}Ca_{0.33}Cr_{0.9}Cu_{0.1}O_{3-\delta}$ (LCCC), has been successfully synthesized with glycine nitrate process (GNP) with a low calcination temperature of 1,000 °C. The XRD analysis and Rietveld refinement displayed that LCCC crystallized in orthorhombic, *Pbnm* space group. The cell parameters, volume and phase are similar to that of reported LaCaCr-based materials. This shows the promise of material to utilize as a Ni-free anode in solid oxide fuel cells especially when methane is used as fuel. Cu-doping in LCCC is expected to enhance the direct electrochemical oxidation which can prevent coke formation. SEM revealed that LCCC is a porous material with the grain size 1-3 μm which shows promise as an anode for SOFC application. The LCCC can be fabricated with electrolyte and cathode into a complete fuel cell and test the cell performance to examine the power density. The microstructure of the fuel cell can also be carried out to observe the cell before and after testing with carbon-containing fuel in case of coke formation investigation. The study of SOFC material with methane is interesting in terms of the use of alternative fuel to hydrogen since methane and other hydrogen-rich fuel can be accessed in biomass gasification or biogas. Therefore, the material development in SOFC is crucial in the future application of LCCC in syngas-fuelled SOFC.

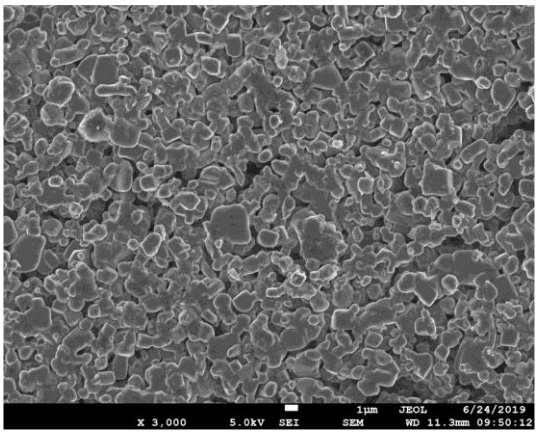

Fig. 4 - SEM image of $La_{0.67}Ca_{0.33}Cr_{0.9}Cu_{0.1}O_{3-\delta}$ at magnification of 3,000

Table 2 - Compositional distribution of $La_{0.67}Ca_{0.33}Cr_{0.9}Cu_{0.1}O_{3-\delta}$ from EDX

Element	Composition	EDX wt %	Formula wt %
La	0.67	46.76	43.73
Ca	0.33	6.93	1.88
Cr	0.9	22.76	21.99
Cu	0.1	1.77	9.85
O	3	21.79	22.55
Total	-	100	100

Acknowledgement

N. Radenahmad is thankful to Universiti Brunei Darussalam for sponsoring the UBD graduate scholarship to do Ph.D. at Brunei Darussalam. It is thankful to Muhammad Saqib for the assistance at Sejong University and Dr. Md. Aminul Islam, Geological Sciences, UBD, for the access to SEM facility. This work was also partially funded from the research grant UBD/OVAORI/CRGWG(006)/161201.

References

[1] Ahmed, A., Abu Bakar, M.S., Azad, A.K., Sukri, R.S., & Mahlia, T.M.I., (2018). Potential thermochemical conversion of bioenergy from Acacia species in Brunei Darussalam: A review. Renewable and Sustainable Energy Reviews, 82, 3060–3076

[2] Radenahmad, N., Abdul Rahman, I.S., Haji Morni, N.A., & Azad, A.K., (2018). Acacia-Polyethylene Terephthalate Co- Gasification as Renewable Energy Resource. International Journal of Renewable Energy Research, 8(3), 1612–1620

[3] Radenahmad, N., Morni, N.A.H., Ahmed, A., Abu Bakar, M.S., Zaini, J., & Azad, A.K., (2018). Characterization of rice husk as a potential renewable energy source. 7th Brunei International Conference on Engineering and Technology 2018 (BICET 2018), 30 (4 pp.)

[4] Ud Din, Z., & Zainal, Z.A., (2016). Biomass integrated gasification-SOFC systems: Technology overview. Renewable and Sustainable Energy Reviews, 53, 1356–1376
[5] Mirzababaei, J., Chuang, S., Mirzababaei, J., & Chuang, S.S.C., (2014). $La_{0.6}Sr_{0.4}Co_{0.2}Fe_{0.8}O_3$ Perovskite: A Stable Anode Catalyst for Direct Methane Solid Oxide Fuel Cells. Catalysts, 4(2), 146–161
[6] Aravind, P. V., Woudstra, T., Woudstra, N., & Spliethoff, H., (2009). Thermodynamic evaluation of small-scale systems with biomass gasifiers, solid oxide fuel cells with Ni/GDC anodes and gas turbines. Journal of Power Sources, 190(2), 461–475
[7] Abdalla, A.M., Hossain, S., Azad, A.T., Petra, P.M.I., Begum, F., Eriksson, S.G., & Azad, A.K., (2018). Nanomaterials for solid oxide fuel cells: A review. Renewable and Sustainable Energy Reviews, 82, 353–368.
[8] Smith, B.H., & Gross, M.D., (2011). A Highly Conductive Oxide Anode for Solid Oxide Fuel Cells. Electrochemical and Solid-State Letters, 14(1), B1–B5
[9] Huang, Y.H., Dass, R.I., King, Z.L., & Goodenough, J.B., (2006). Double perovskites as anode meterials for solid-oxide fuel cells. Science, 312(5771), 254–257
[10] Zhang, P., Huang, Y.-H., Cheng, J.-G., Mao, Z.-Q., & Goodenough, J.B., (2011). Sr_2CoMoO_6 anode for solid oxide fuel cell running on H2 and CH4 fuels. Journal of Power Sources, 196(4), 1738–1743
[11] Bebelis, S., Neophytides, S., Kotsionopoulos, N., Triantafyllopoulos, N., Colomer, M.T., & Jurado, J., (2006). Methane oxidation on composite ruthenium electrodes in YSZ cells. Solid State Ionics, 177(19–25), 2087–2091
[12] Zha, S., Cheng, Z., & Liu, M., (2005). A Sulfur-Tolerant Anode Material for SOFCs $Gd_2Ti_{1.4}Mo_{0.6}O_7$. Electrochemical and Solid-State Letters, 8(8), A406–A408
[13] Gorte, R.J., Kim, H., & Vohs, J.M., (2002). Novel SOFC anodes for the direct electrochemical oxidation of hydrocarbon. Journal of Power Sources, 106(1–2), 10–15
[14] Ye, X.F., Huang, B., Wang, S.R., Wang, Z.R., Xiong, L., & Wen, T.L., (2007). Preparation and performance of a Cu-CeO_2-ScSZ composite anode for SOFCs running on ethanol fuel. Journal of Power Sources, 164(1), 203–209
[15] Goodenough, J.B., & Huang, Y.-H., (2007). Alternative anode materials for solid oxide fuel cells. Journal of Power Sources, 173(1), 1–10
[16] Azad, A.K., Mellergård, A., Eriksson, S.-G., Ivanov, S.A., Yunus, S.M., Lindberg, F., Svensson, G., & Mathieu, R., (2005). Structural and magnetic properties of $LaFe_{0.5}Cr_{0.5}O_3$ studied by neutron diffraction, electron diffraction and magnetometry. Materials Research Bulletin, 40(10), 1633–1644
[17] Azad, A.K., Eriksson, S.-G., & Irvine, J.T.S., (2009). Structural, magnetic and electrochemical characterization of $La_{0.83}A_{0.17}Fe_{0.5}Cr_{0.5}O_{3-\delta}$ (A = Ba, Ca) perovskites. Materials Research Bulletin, 44(7), 1451–1457
[18] Sauvet, A.L., & Fouletier, J., (2001). Electrochemical properties of a new type of anode material $La_{1-x}Sr_xCr_{1-y}Ru_yO_{3-\delta}$ for SOFC under hydrogen and methane at intermediate temperatures. Electrochimica Acta, 47(6), 987–995
[19] Caillot, T., Gélin, P., Dailly, J., Gauthier, G., Cayron, C., & Laurencin, J., (2007). Catalytic steam reforming of methane over $La_{0.8}Sr_{0.2}CrO_3$ based Ru catalysts. Catalysis Today, 128(3-4 SPEC. ISS.), 264–268
[20] Tao, S., & Irvine, J.T.S., (2004). Synthesis and Characterization of $(La_{0.75}Sr_{0.25})Cr_{0.5}Mn_{0.5}O_{3-\delta}$, a Redox-Stable, Efficient Perovskite Anode for SOFCs. Journal of The Electrochemical Society, 151(2), A252–A259
[21] Liu, J., Madsen, B.D., Ji, Z., & Barnett, S.A., (2002). A Fuel-Flexible Ceramic-Based Anode for Solid Oxide Fuel Cells. Electrochemical and Solid-State Letters, 5(6), A122–A124
[22] Vashook, V., Vasylechko, L., Zosel, J., & Guth, U., (2003). Synthesis, crystal structure, and transport properties of $La_{1-x}Ca_xCr_{0.5}Ti_{0.5}O_{3-\delta}$. Solid State Ionics, 159(3–4), 279–292
[23] Rodriguez-Carvajal, J., (1993). Recent advances in magnetic structure determination by neutron powder diffraction + FullProf. Physica B: Condensed Matter, 192(1–2), 55
[24] Hossain, S., Abdalla, A.M., Jamain, S.N.B., Zaini, J.H., & Azad, A.K., (2017). A review on proton conducting electrolytes for clean energy and intermediate temperature-solid oxide fuel cells. Renewable and Sustainable Energy Reviews, 79, 750–764
[25] Shannon, R.D., (1976). Revised Effective Ionic Radii and Systematic Studies of Interatomic Distances in Halides and Chalcogenides. Acta Crystallographica Section A, 32(5), 751–767